

# Shaping centromeres to resist mitotic spindle forces

Josh Lawrimore and Kerry Bloom\*

## ABSTRACT

The centromere serves as the binding site for the kinetochore and is essential for the faithful segregation of chromosomes throughout cell division. The point centromere in yeast is encoded by a ~115 bp specific DNA sequence, whereas regional centromeres range from 6–10 kbp in fission yeast to 5–10 Mbp in humans. Understanding the physical structure of centromere chromatin (pericentromere in yeast), defined as the chromatin between sister kinetochores, will provide fundamental insights into how centromere DNA is woven into a stiff spring that is able to resist microtubule pulling forces during mitosis. One hallmark of the pericentromere is the enrichment of the structural maintenance of chromosome (SMC) proteins cohesin and condensin. Based on studies from population approaches (ChIP-seq and Hi-C) and experimentally obtained images of fluorescent probes of pericentromeric structure, as well as quantitative comparisons between simulations and experimental results, we suggest a mechanism for building tension between sister kinetochores. We propose that the centromere is a chromatin bottlebrush that is organized by the loop-extruding proteins condensin and cohesin. The bottlebrush arrangement provides a biophysical means to transform pericentromeric chromatin into a spring due to the steric repulsion between radial loops. We argue that the bottlebrush is an organizing principle for chromosome organization that has emerged from multiple approaches in the field.

**KEY WORDS:** Bottlebrush, Centromere, Mitosis, Polymer models, Kinetochore

## Introduction

The centromere is the primary constriction in a condensed mitotic chromosome and is the binding site for the kinetochore complex (Musacchio and Desai, 2017). Sister chromatids are mechanically linked through the centromere, but the exact nature of this mechanical linkage remains poorly understood. However, the importance of the topological organization of this region during mitosis throughout eukaryotic evolution is well established. Correct bipolar attachment of sister chromatids to the mitotic spindle leads to microtubule (MT)-based tension between sister kinetochores. Centromere tension, which can be visualized by light microscopy as centromere stretching (Maresca and Salmon, 2009; Pearson et al., 2001; Waters et al., 1996), arises when microtubules attached to sister kinetochores shorten, exerting a pulling force on the centromere. The kinetochore complexes that are bound to sister chromatids are mechanically linked through the centromere DNA. The kinetochore is composed of ~100 different proteins, organized into five to six major complexes (Biggins, 2013; Musacchio and Desai, 2017). Using quantitative light microscopy and *in vivo*

two-color fluorescence microscopy, the protein stoichiometry and architecture of the yeast kinetochore has been determined at nanometer resolution (Joglekar et al., 2009, 2006). The geometry of the core structure proved to be remarkably similar to that found in mammalian kinetochores, indicating that kinetochore structure is conserved in eukaryotes (Joglekar et al., 2009, 2006; Kukreja et al., 2020; Wan et al., 2009; Lawrimore et al., 2011). There has also been significant progress in mapping the tension-sensitive linkages within the stiff kinetochore that endow it with exquisite sensitivity to translate the critical information provided by tension to cell cycle progression (Joglekar and Kukreja, 2017; Musacchio and Ciliberto, 2012; Salmon and Bloom, 2017).

Despite the conserved kinetochore structure, there is striking diversity in centromere organization. Centromere DNA spans several orders of magnitudes throughout evolution, ranging from the 120 base pair point centromeres in budding yeast to the several megabases of the regional centromere in human centromeres (reviewed in Talbert and Henikoff, 2020; Miga and Sullivan, 2021; Mellone and Fachinetti, 2021) (see Box 1). The point centromere is the site of kinetochore assembly, while kinetochores assemble on only a small fraction of the mass of DNA in a regional centromere (Box 1). Strikingly, the apparent disparity in DNA size belies the highly conserved distance between separated sister kinetochores in organisms as diverse as yeast, worms, flies, flower moths, plants, horses and humans (800 to 1000 nm; see Box 1 and table therein) (Lawrimore and Bloom, 2019).

This Opinion will highlight the recent advances in the function of the centromere DNA during mitosis, with the aim of deducing the organizational physical principles that confer centromeres with the ability to withstand MT-based forces.

## Forces on the centromere

The mitotic spindle comprises MTs that extend between the two MT-organizing centers, or spindle poles (polar MTs). MTs are dynamic polymers that undergo cycles of growth and shortening, termed dynamic instability (Mitchison and Salmon, 2001). Kinetochores capture MTs (kinetochore MTs) and continue this process until kinetochores and their sister chromatids become oriented between the two spindle poles. As MTs remain dynamic, centromeres stretch in response to phases of MT growth and shortening (Maresca and Salmon, 2009; Pearson et al., 2001; Waters et al., 1996). Incorrect monopolar attachment, where only one of the sister kinetochores is attached, does not lead to centromere tension. In a classic series of elegant micromanipulation experiments with grasshopper chromosomes and force-calibrated needles performed half a century ago, it was established that MT attachments to kinetochores are unstable unless the kinetochore is under tension (Henderson and Koch, 1970; Nicklas, 1988; Nicklas and Koch, 1969). Subsequent work with phosphorylation-sensitive probes revealed that tension is monitored within the kinetochore (Nicklas et al., 1995), laying the groundwork for the site of action of the spindle assembly checkpoint. Moreover, a lack of tension at the kinetochore delays continuation of mitosis, giving cells time to correct chromosome attachment defects

Department of Biology, 623 Fordham Hall CB#3280 133 Medical Drive, University of North Carolina at Chapel Hill, Chapel Hill, NC 27599-3280, USA.

\*Author for correspondence (kerry\_bloom@unc.edu)





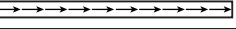
 K.B., 0000-0002-3457-004X

### Box 1. Centromere diversity

Centromere DNA varies in size from 0.1 to thousands of kilobase pairs depending on the species (see table). Point centromeres (0.1 kbp) are the site of kinetochore assembly in budding yeast (Bloom and Carbon, 1982), whereas in regional centromeres, only a fraction of centromere DNA interacts with the kinetochore complex (Cleveland et al., 2003). Arrows in the table denote regions of hierarchical DNA repeats in regional centromeres. In contrast to the variance in centromere DNA size (in kb) across phylogeny, the distance (in microns) between sister kinetochores is remarkably conserved [in budding yeast, *S. cerevisiae* (Lawrimore et al., 2016; Yeh et al., 2008); worm, *C. albicans* (Maddox et al., 2006); fission yeast, *S. pombe* (Ding et al., 1993); fly, *D. melanogaster* (Venkei et al., 2012); and human, *H. sapiens* (Salmon et al., 1976)]. Furthermore, the area between sister kinetochores in budding yeast ( $2\pi r h \approx 0.6 \mu\text{m}^2$ ) is

comparable to estimates of the size of mammalian kinetochores ( $\approx 0.4 \mu\text{m}^2$ ) (Cherry et al., 1989). The region flanking the point centromere in budding yeast has a threefold enrichment in cohesin and condensin. This region, denoted as pericentromere (indicated in red in the table), spans  $\sim 30\text{--}50$  kb surrounding the centromere, bounded by sites of convergent gene transcription (Paldi et al., 2020). The total amount of pericentromeric chromatin in metaphase in budding yeast is  $\sim 1\text{--}1.6$  Mbp (16 chromosomes  $\times 30\text{--}50$  kbp  $\times$  two sister strands), comparable to the 1–5 Mbp lengths of  $\alpha$ -satellite DNA in a mammalian centromere. The mammalian centromere is therefore structurally analogous to the yeast centromere (125 bp) and flanking pericentromere (30–50 kb/chromosome). In mammals, the pericentromere is defined as the chromatin region flanking the primary constriction (i.e. centromere) (Cleveland et al., 2003), and is distinct from the yeast pericentromere described herein.

### Centromere size and kinetochore separation from fungi to human

	Centromere DNA size	Schematic of point versus regional centromere	Kinetochore separation in mitosis
<i>S. cerevisiae</i>	0.125 kb		800 nm
<i>C. albicans</i>	3–4 kb		$\sim 800$ nm
<i>S. pombe</i>	10 kb		$\sim 1000$ nm
<i>D. melanogaster</i>	200–500 kb		$\sim 1000$ nm
<i>H. sapiens</i>	500–1500 kb		$\sim 1000$ nm

before anaphase (Li and Nicklas, 1995). Thus, tension at the kinetochore is a primary source of information to ensure error-free chromosome segregation (Henderson and Koch, 1970; Li and Nicklas, 1995; Nicklas and Koch, 1969).

To create tension, kinetochore MT-based pulling forces from one spindle pole must be balanced by opposing forces from kinetochore MTs originating from the other spindle pole. The centromere is the mechanical link between sister kinetochores. Based on the change in distance between sister kinetochores as a function of MT growth and shortening, the centromere operates as a mechanical spring. Insight into the structure and function of the centromere spring was enabled with the ability to visualize specific DNA foci in live cells (Robinett et al., 1996; Straight et al., 1996). A segment of the centromere was visualized through the insertion of the lac operator sequence from bacteria (lacO) bound to lac repressor fused to GFP (LacI-GFP), generating so-called fluorescent reporter operator spots (FROS). Sister centromere FROS are dynamic, exhibiting cycles of separation and recoil (Goshima and Yanagida, 2000; He et al., 2000; Pearson et al., 2001; Tanaka et al., 2000). By using imaging and quantitative approaches, the spring-like property of the centromere has been found to be tunable and to undergo a mechanical maturation process in metaphase (Harasymiw et al., 2019; Mukherjee et al., 2019; Stephens et al., 2011). Forces can be inferred from the thermal fluctuation of the DNA polymer (Chacon et al., 2014; Lawrimore et al., 2015; Verdaasdonk et al., 2013). Using simplifying assumptions such as measuring the spring constant of an optical trap, the spring constant ( $k_s$ ) can be inferred from the variance in FROS fluctuations ( $k_s = k_B T / \text{variance}$ ;  $k_B$ , Boltzmann's constant;  $T$ , temperature). A recent study manipulated MT-based motors and MT-binding proteins to demonstrate that centromere tension is calibrated to MT-based pulling forces (Mukherjee et al., 2019).

However, a major question remaining is how the centromere spring is built and maintained. In contrast to the stiff kinetochore,

chromatin is compliant and heterogeneous in its mechanical properties (Kruithof et al., 2009). There are 2 m of DNA in a mammalian cell nucleus ( $\sim 5 \mu\text{m}$  in diameter) and 5 mm of DNA in a yeast cell nucleus ( $\sim 2 \mu\text{m}$  in diameter). The amount of force generated by a mitotic spindle is on the order of piconewtons ( $10^{-12}$  Newtons) (Jannink et al., 1996; Nicklas, 1983), whereas the amount of force required to extend DNA to 70% of its B-form length is in the range of merely femtonewtons ( $10^{-15}$  Newtons) (Bloom, 2008; Bustamante et al., 1994; Marko and Siggia, 1995). Therefore, 3 kb of DNA will extend to 700 nm with femtonewtons of force, while the centromere spring must be able to resist up to piconewtons of MT-based forces. Thus, were DNA itself to be the spring, there could only be a few thousand base pairs between sister kinetochores. Considering we can introduce 10 kb of lacO DNA (FROS) into the centromere with little consequence on spring function, there must be a higher order organizing principle governing the properties of the spring. The question becomes how is tensile stiffness generated with a 'floppy' chromatin substrate? Moreover, how is the centromere tuned and how does it mature during mitotic onset?

### Centromere structure

Elucidating centromere biology from its sequence in organisms with regional centromeres has proven challenging due to the difficulty in assembling accurate sequence reads through megabases of DNA repeats. In addition, deducing the higher-order structure of centromeres was challenging owing to the disorder that is inherent in kilo- to mega-base pairs of chromatin. The sequencing challenge has largely been met with innovation in alignment algorithms, read-depth and ultra-long-read sequencing efforts (Miga et al., 2020). Likewise, there has been a revolution in our understanding of the higher-order structure and organization of chromosomes in the past decade. Several recent approaches (3C, Hi-C, ChromEMT and super-resolution microscopy) have revealed that a chromosome is a disordered array of loopy fibers that emanate from an axial core

(Dekker et al., 2013; Dostie and Bickmore, 2012; Ou et al., 2017). The hierarchical models of chromosome folding, building from 11 nm beads on a string (nucleosomes) to 30 nm solenoids and higher-order fibers are not borne out in recent 3D and live-cell studies (Ou et al., 2017). In the 1970s, Paulson and Laemmli observed DNA loops in chromosome spreads of isolated mammalian cells; in metaphase, these loops emanate from a protein-rich chromosome scaffold (Paulson and Laemmli, 1977). Subsequently, the chromosome scaffold was found to be enriched in strand passage enzymes, such as topoisomerase II and the structural maintenance of chromosomes (SMC) proteins condensin and cohesin (Earnshaw et al., 1985; Hirano, 2006). SMC proteins assemble into multi-subunit complexes that adopt a ring-like conformation. The backbone of the ring is formed by the SMC proteins themselves (MukB in bacteria; Smc2 and Smc4 in *Saccharomyces cerevisiae* condensin, and Smc1 and Smc3 in *S. cerevisiae* cohesin). In eukaryotes, the SMC monomer is folded in an antiparallel coiled coil. Two monomers associate to form a hinge at one end, and an ATP-binding-domain at the other end. Closure of the ring at the head domain is carried out by proteins known as kleisins, including Scc1 (also known as Mcd1) and Brn1. Each dimer is associated with additional proteins, for example, Ysc4, Ycg1, Scc3 (also known as Irr1), Rad61 and Pds5, at the head domain to form a functional complex *in vivo*. In bacteria, the SMC coiled coils are bound by ScpA and ScpB (Mascarenhas et al., 2002).

DNA loops are tethered at their base to the condensin-enriched chromosome scaffold. Loops are a natural consequence of the entropic fluctuations and excluded-volume interactions of tethered polymer chains in a confined space, such as the 5  $\mu\text{m}$  long DNA in the 2  $\mu\text{m}$  yeast nucleus (Vasquez et al., 2016). In addition, energy-requiring processes are also involved in loop formation. Indeed, SMC proteins, which bind and hydrolyze ATP, have been shown to have loop-extrusion potential (Alipour and Marko, 2012). Moreover, condensin has garnered attention based on recent reports that it is a DNA translocase (Terakawa et al., 2017). Early single-molecule manipulation experiments found condensin to be capable of compacting DNA (Strick et al., 2004), presaging recent efforts demonstrating the ability of condensin to extrude loops (Ganji et al., 2018; Kong et al., 2020). The extrusion rate is highly sensitive to force such that sub-piconewton forces are sufficient to stall the process (0.4 pN) (Ganji et al., 2018; Kong et al., 2020; Strick et al., 2004). To provide a frame of reference for the 'strength' of loop extrusion, the extrusion stall force is well below that required to unwind nucleosomal DNA (2 pN) (Yan et al., 2007). Thus, any higher order looping configuration is poised for remodeling when challenged with enzymes that can displace nucleosomes.

Long chain polymers such as chromosomes are challenging to model due to the wide range of length and time scales involved in their dynamics, as well as the vast number and variety of polymer configurations (Underhill and Doyle, 2004). The large number of configurations contributes significantly to the entropy and is the basis for the entropic spring-like behavior of DNA. Forces acting on chromosomal DNA to deform it in any way are constantly working against an entropic restoring force that is characteristic of polymeric systems. Even with robust algorithms for chromosome behavior, the complexity in the models must necessarily be reduced compared to what is observed *in vivo*. The dynamics of chromosomes can be modeled using a bead-spring polymer model where the chromosomes are represented by interacting beads connected via springs as described by a worm-like chain (WLC) force law (Marko and Siggia, 1995). Representing the restoring force with springs and modeling the polymer as a bead-spring chain has proven invaluable

to understanding chromosome behavior (de Gennes, 1979; Doi and Edwards, 1986; Goloborodko et al., 2016; Mirny, 2011). These polymer models do remarkably well in capturing the large-scale folding and organizational principles derived from population studies (Lawrimore et al., 2016, 2017a; Verdaasdonk et al., 2013), as well as dynamic changes upon transcriptional activation, DNA damage and sequestration of the rDNA into the nucleolus (Bystricky et al., 2004; Dekker and Misteli, 2015; Dion and Gasser, 2013; Lawrimore et al., 2017a, 2021).

A second impetus for implementing polymer models is building intuition in an environment foreign to our own. We generate intuition based upon our observations. Unfortunately, the world we live in (inertia dominated) is completely inappropriate for the viscosity-dominated world at the scale of the cell. Chromosome motion is also counter-intuitive. While we can readily understand the random walk of an individual, it is much more difficult to conceptualize that walk when we are watching an individual (i.e. a gene) that is but one of thousands of individuals (genes) linked together in a long chain chromosome polymer. An example that emphasizes the counter-intuitive aspect of long chain polymers is the segregation of polymers from one another in a confined space (Jun and Mulder, 2006). The entropic penalty of strand mixing in a small space is sufficient to drive two polymers apart from one another. A second example is the generation of loops by a translocase walking along a floppy substrate (Lawrimore et al., 2017b; He et al., 2020). A simple stepping motor will generate loops if stepping is not restricted to the linear order of beads but rather to the spatial relationship of beads in the chain. The predictions from these models, while counterintuitive, provide simple explanations for substantial biological concepts.

To maximize the utility of the bead-spring models, we translated the models into experimental images (Gardner et al., 2010; Quammen et al., 2008). We computationally marked individual beads of the chain as fluorescent and spread the light from those beads using a defined algorithm as it passes through an objective (point spread function). This enables direct comparison of the model to microscope images of live cells (Quammen et al., 2008). In this way, the models described below provide a means to build intuition based on the behavior of polymers in a highly viscous environment, which is subject to thermal and entropic forces that are otherwise very difficult to interrogate. This approach further allows us to explore a range of model parameters and distinguish among multiple hypotheses (Hult et al., 2017; Lawrimore et al., 2016; Stephens et al., 2013b,c).

### Centromere cohesion

The tensile strength of centromeric chromatin is dictated in large part by cohesin and condensin (Lawrimore et al., 2018, 2015). Because cohesin holds sister chromatids together, it was initially assumed that cohesin-based tethers were responsible for resisting outward MT-pulling forces (Michaelis et al., 1997; Nasmyth and Haering, 2009) (Fig. 1). Cohesin (Smc1 and Smc3) is essential for nuclear division (Strunnikov et al., 1993), and loss of function alleles lead to precocious separation of sister chromatid arms (Strunnikov et al., 1995, 1993). However, the function of cohesin at the point centromere of budding yeast is not as simple as a ring holding two DNA strands together, as sister kinetochore complexes are separated by 800 nm during mitosis (Pearson et al., 2001). In addition to cohesin, condensin (Smc2 and Smc4), essential for chromosome condensation (Strunnikov et al., 1995), plays a key role at the budding yeast pericentromere. Perturbing condensin function by introducing a temperature-sensitive mutation increases

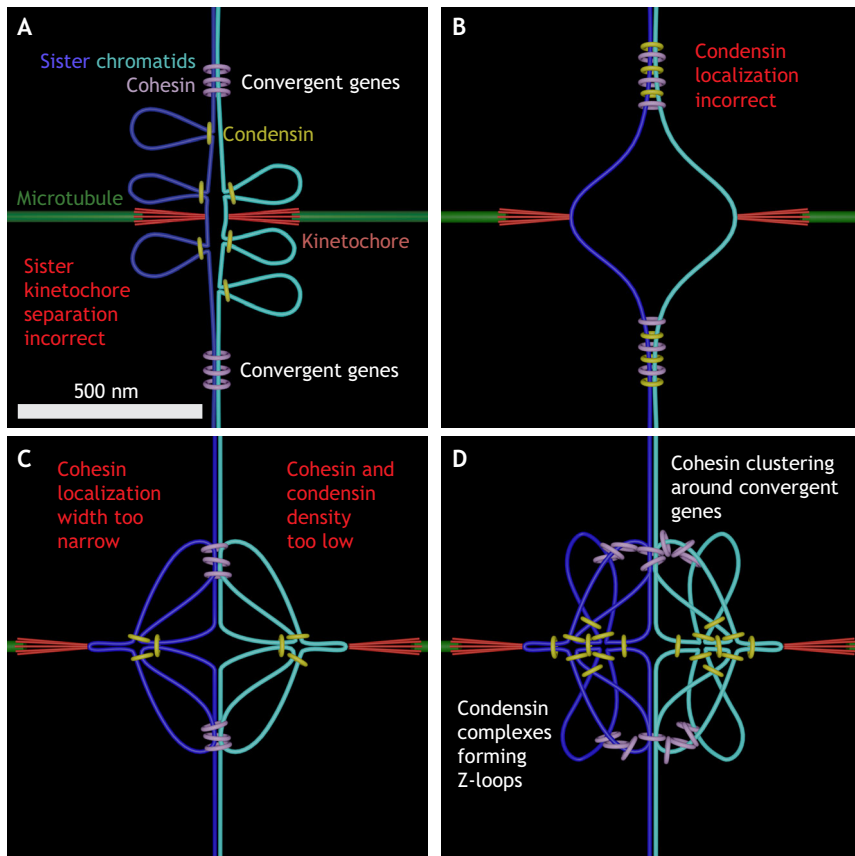


**Fig. 1. Proposed centromere configurational states.** (A) The cohesion model of a point centromere. Only a single pair of sister chromatids (light and dark blue) are shown for clarity. Cohesin (lilac) holds sister chromatids together at sites of convergently transcribed genes. Cohesin is a  $\sim 50$  nm ring. The model does not account for the distance between sister kinetochores (800 nm), nor the position of condensin (yellow) to be aligned along the microtubule (green) axis. (B) The V model of a point centromere (Paldi et al., 2020). This model accurately depicts the separation of sister kinetochore complexes but does not account for the spatial segregation of cohesin and condensin. (C) The C-loop model correctly predicts the localization of cohesin and condensin, as well as that of DNA loops and kinetochores. However, the density of cohesin and condensin are too low, resulting in too few SMC complexes to account for the observed density of cohesin and condensin. In the budding yeast pericentromere, cohesin and condensin are enriched threefold over their typical density of one cohesin per 10 kb and one condensin per 10 kb. (D) The bottlebrush model of a point centromere (Lawrimore et al., 2016, 2015). This model correctly predicts the physiologically determined stoichiometry of cohesin and condensin within the pericentric region and incorporates the recent discoveries of condensin-mediated Z-loops and cohesin clustering.

spindle length and destabilizes spindle length during metaphase of mitosis (Stephens et al., 2011). Condensin perturbation also results in increased stretching of a fluorescently labeled, bi-oriented, dicentric plasmid that serves as an *in vivo* proxy of separated sister chromatids (Lawrimore et al., 2018; Stephens et al., 2011). Taken together, these results demonstrate that both cohesin and condensin are important for the stability and resistivity of sister chromatid cohesion during metaphase.

Early models for centromeric cohesin placed sister-chromatid linkages at the centromere itself (Fig. 1A,B). However, as more information has accrued, including chromatin immunoprecipitation mapping of cohesin and condensin, 3D contact maps (3C and Hi-C) of yeast chromosomes, cell biology of FROS, cohesin and condensin, as well as quantitative models of DNA polymer behavior, the simple models were found to be insufficient to account for the spectrum of experimental evidence. More recent models, which are not mutually exclusive, include sister-chromatid linkages distal to the centromere at sites of convergent genes and polymer-based bottlebrush models that invoke DNA looping as a major feature of centromeric chromatin (Fig. 1A–D).

There are several issues with models that rely on cohesin tethering of sister chromatids at the centromere (Fig. 1). First, the distance between separated sister kinetochores is  $\sim 800$  nm in budding yeast and  $\sim 1000$  nm in mammalian cells (Pearson et al., 2001; Salmon, 1975). As the cohesin ring is only  $\sim 40$  nm in diameter (Haering et al., 2002), this implies that cohesin cannot directly bridge the distance between sister centromeres together, this raises the question of how tension is maintained over the 800 to 1000 nm of centromeric chromatin between sister kinetochores (compare Fig. 1A and Fig. 1B).

Second, the length scale of sister kinetochore separation ( $\sim 800$  nm) is an order of magnitude larger than the length scale over which DNA is stiff (50 nm). Models for centromere cohesin must take into account the mechanical properties of DNA. The mechanics of naked DNA can be explained by a simple elastic model, the WLC (Marko and Siggia, 1995). The WLC describes DNA using a single parameter  $L_p$  (persistence length), which is defined mathematically as the length scale over which the tangential vectors along the DNA become uncorrelated ( $L_p$  for DNA = 50 nm, corresponding to  $\sim 150$  bp) (Howard, 2001; Rubinstein and Colby, 2003). This indicates that the ends of a  $\sim 150$  bp DNA fragment are roughly coordinated, and they become completely independent with increasing fragment length, resulting in a floppy chain. A floppy chain adopts the conformation of a random coil, with one consequence being the relatively weak force required to extend it. Furthermore, only when DNA is elongated to  $\sim 70\%$  of its B-form length, when it is well out of the thermodynamically preferred conformation of a random coil, will it provide significant resistance to further extension. If DNA was acting as a spring between separated sister kinetochores, the length required to resist pulling forces exerted by the MTs would be on the order of 3 to 4 kb ( $\sim 700$  to 1000 nm) (Dewar et al., 2004). However, there is far too much DNA between sister kinetochores, by several orders of magnitude, in organisms with either point or regional centromeres, for DNA alone to act as an effective spring. Simple displacement of cohesin from the centromere (Fig. 1B) does not help us understand the path of DNA over the micron length scale between sister kinetochores.

Third, there is the challenge in deriving organizational principles from the statistics of population studies of fixed cells (e.g. chromatin immunoprecipitation, 3C and Hi-C) into an individual cell in which chromosomes are constantly wiggling and writhing within a very

active nucleoplasm. The complexity in deducing mechanism from population statistics is exemplified in the analysis of cohesin and condensin from population studies versus live-cell analysis (Vasquez and Bloom, 2014). Analysis of chromatin immunoprecipitation studies reveals highly overlapping patterns of condensin (Smc4) and cohesin (Scc1) throughout the centromere and surrounding region (Blat and Kleckner, 1999; D'Ambrosio et al., 2008; Glynn et al., 2004; Megee et al., 1999). In contrast, single-cell analysis reveals a non-overlapping distribution of condensin and cohesin. Pericentric condensin (Smc4) is localized along the central spindle axis between sister kinetochores (Stephens et al., 2011), while cohesin (Smc3) is radially displaced from the spindle axis (Lawrimore et al., 2018; Stephens et al., 2013b; Yeh et al., 2008). The apparent discrepancy between the fixed- and live-cell data can be reconciled by considering DNA dynamics. DNA chains, like all matter in the cell, are in a state of constant thermal fluctuation. Even though cohesin and condensin in the pericentromere are spatially segregated, they bind on average all DNA segments in the pericentromere, as different regions of DNA constantly explore the space between sister kinetochores. Cohesin and condensin do not bind, on average, all the pericentromeric DNA in a single cell, but when a population of cells is sampled, as is the case in chromatin immunoprecipitation (ChIP) or Hi-C, the sum of all configurational states of DNA is realized. Therefore, models of centromere structure must incorporate the behavior of single chromatin chains in live cells together with statistical data from population studies and biophysical observations from reconstitution experiments.

Fourthly, spindle MTs are cylindrically organized (~250 nm in diameter and 1500 nm long in metaphase in budding yeast) (Winey and Bloom, 2012), but cohesin is distal to the central MT axis (Lawrimore et al., 2018; Stephens et al., 2013b; Yeh et al., 2008). Centromeric cohesin (Smc3–GFP) appears as a cylinder (~500 nm diameter and 550 nm long) that encircles the central spindle MTs. The cylindrical geometry is a consequence of the spread of fluorescence from ~300 cohesin–GFP complexes (Lawrimore et al., 2011) that are evenly distributed around the spindle axis (Yeh et al., 2008) (Stephens et al., 2013c). This position of cohesin is incompatible with models that posit cohesin as the sole spring that opposes MT-pulling forces (Fig. 1A,B). Instead, cohesin and condensin have distinct roles to enable pericentric chromatin to stably withstand pulling forces from MTs. Recent *in vitro* studies of budding yeast cohesin and condensin reveal that condensin complexes can extrude loops (Ganji et al., 2018; Terakawa et al., 2017) and generate loop-in-loop structures, called Z-loops (Kim et al., 2020), while cohesin complexes that are bound to DNA are capable of clustering together given a sufficient DNA length (>3 kb) and cohesin concentration (Ryu et al., 2021) (Fig. 1D). The ability of condensin to extrude Z-loops may be the underlying cause of radial loops of chromatin and the basis for its axial localization.

Finally, the motion of non-sister chromatids (chromosomes 11 and 15) is correlated (Stephens et al., 2013c). Using dual labeled FROS to interrogate the motion of pericentromeres adjacent to centromeres from chromosomes XI and XV (CEN11 and CEN15, respectively), we were able to follow the motion of different pericentromeres in the same cell. Different pericentric chromatids exhibited coordinated motion and stretching (length changes from foci to a linear element), indicative of physical linkages between non-sister strands (Stephens et al., 2013c). Coordinated motion is dependent on condensin, while coordinated stretching depends on cohesin (Stephens et al., 2013c). Potential mechanisms that could account for the coordinated behavior of non-sister strands include

the formation of DNA–cohesin condensates via bridging-induced phase separation (Ryu et al., 2021) and/or the ability of cohesin to form slip links on DNA (Borrie et al., 2017; Stigler et al., 2016). Protein complexes that function as slip rings (or molecular pulleys) provide a mechanism to distribute tension from one location to the entire network (Okumura and Ito, 2001). Cohesin has the physical attributes of a slip ring and might contribute to coordinated movements as a means to regulate centromere elasticity. Likewise, these bridging and/or cross-linking functionalities provide a mechanism to sequester sub-domains in the nucleus (e.g. nucleolus; Hult et al., 2017) as an alternative means to coordinate non-sister strands.

### **Bottlebrush model of the centromere**

The observations outlined above indicate that neither cohesin nor a DNA spring account for the resistance of the centromere to pulling forces, raising the question of how, then, does the pericentromeric chromatin (hereafter pericentromere) organization provide the requisite tensile element?

A major advance in answering this question was the proposal and validation of a bottlebrush model for the pericentromere (Lawrimore et al., 2016, 2015) (depicted in Fig. 2A,B). A molecular bottlebrush resembles the laboratory brushes used to wash test tubes. The brush has a long backbone (primary axis) populated with a dense array of shorter side chains. The distinct feature of the bottlebrush is that steric repulsion between the side chains stretches the primary axis. This configuration provides a mechanism to generate significant tension along the DNA backbone. The magnitude of axial tension is dependent on the density and length of the loops (Lebedeva et al., 2012; Panyukov et al., 2009a,b; Rubinstein and Colby, 2003). The bottlebrush model for centromeres is derived from a synthesis of experimental results, including the localization and enrichment of cohesin and condensin in the pericentromere as determined by ChIP (Blat and Kleckner, 1999; D'Ambrosio et al., 2008; Megee et al., 1999; Weber et al., 2004), the localization of FROS (Anderson et al., 2009; Stephens et al., 2011, 2013c), and cohesin and condensin observed in live cells (Stephens et al., 2013b; Yeh et al., 2008), and cross-linking studies showing the position of DNA loops (Paldi et al., 2020) (Fig. 3). This model is based on the thermodynamic principles of polymer fluctuations and the presence of loop extrusion proteins (condensin) and molecular slip links (cohesin) (Lawrimore et al., 2016, 2015). Such a bottlebrush arrangement of chromosome organization can be seen across different species and is supported by evidence from different experimental approaches, including imaging and computational modeling (Lawrimore et al., 2015), Hi-C (Gibcus et al., 2018) and *in vitro* studies (Elbatsh et al., 2019) (Fig. 2A–C).

### **Experimental validation of the bottlebrush**

Studies using the yeast pericentromere as a model allow us to discern how the bottlebrush is assembled, regulated and disassembled, and thus provide key insights into the physical attributes of eukaryotic chromosomes in general.

In budding yeast, cohesin and condensin are three-fold enriched in pericentromeric chromatin during mitosis as measured by ChIP (D'Ambrosio et al., 2008; Megee et al., 1999; Weber et al., 2004) but occupy spatially distinct regions within the pericentromeric chromatin similar to the spatially distinct regions that contain condensin I and II in mammalian chromosomes (Elbatsh et al., 2019; Gibcus et al., 2018; Stephens et al., 2011, 2013b) (Figs 2B,C and 3). The physical segregation of condensin and cohesin within the pericentromere *in vivo* highlights several key

**A Yeast pericentromere organization**

**B Mammalian mitotic chromosome**

**C Chromosome organization mediated by condensin I and II**

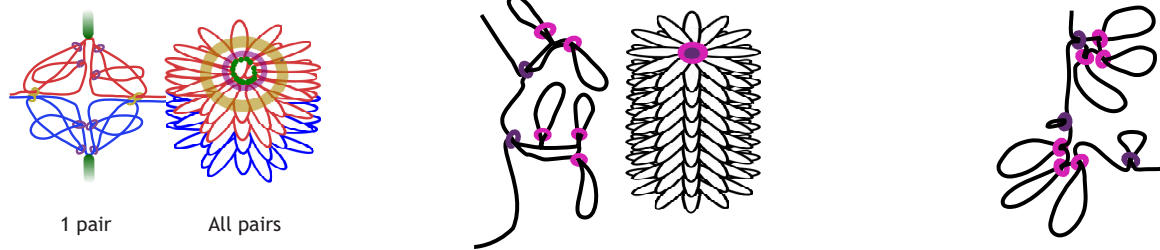


**Fig. 2. Bottlebrush models of chromosomes.** (A) Model of the yeast pericentromere (Lawrimore et al., 2015). A single pair (left) of sister chromatids (red and blue) are attached to microtubules (green). Condensin (purple rings) forms loops along microtubule axis (vertical line connecting microtubules). Cohesin (dark yellow rings) encircles sister chromatids further along the microtubule axis. All 16 pairs of sister chromatids (right) form a bottlebrush upon attachment to microtubules. The primary axis is running north–south (aligned with kinetochore microtubules, shown to the left). The brush is formed upon clustering of the 16 kinetochore pairs shown to the right. The ‘brushes’ of the bottlebrush are secondary loops formed by condensin, perpendicular to the primary spindle axis (north–south). (B) Mammalian mitotic chromosome model (Gibcus et al., 2018). Condensin-II (purple rings) and condensin-I (pink rings) form a nested loop structure (left). The entire mitotic chromosome (right) forms a bottlebrush, similar in structure to the yeast pericentromere. (C) The role of condensin I and II in chromosome organization as proposed in Elbatsh et al. (2019). Condensin I and II are color-coded as in B.

points. First, ChIP experiments identify the position of a given protein (condensin or cohesin) averaged over a large population of cells. The position of condensin and cohesin in individual cells can be reconciled with ChIP data based upon predictions from models shown in Figs 1 and 3. In the case of the bottlebrush model, what may be a side chain in the bottlebrush in one cell can be the primary axis in another cell. Condensin binding to the primary axis and cohesin binding to the side chains will therefore map to the same sequences when these binding modalities are averaged over millions of cells, but they exhibit non-overlapping positions in individual cells.

The spindle imposes a physical constraint that forces the bases of DNA loops to lie along the spindle axis, which means that the tips of

the loops are forced away from the axis. Cohesin is displaced from the central spindle axis and appears as a barrel surrounding the spindle MTs (Fig. 3, experimental and simulated Smc3–GFP images). The simplest model of a diffusible protein ring (slip-link) that encircles one strand of DNA (cohesin) gives rise to a cylindrical arrangement of cohesin that phenocopies the experimentally observed position (Lawrimore et al., 2016). The bottlebrush model predicts this position as the thermodynamically favored site within the DNA loops (Fig. 3B). Through iterations of model parameters, we found that the size of the DNA loops dictates the diameter of the pericentric cohesin barrel (Fig. 3, end-on view of Smc3, experimental and simulated) (Lawrimore et al., 2016). The cohesin complex diffuses to the most entropically favored position,

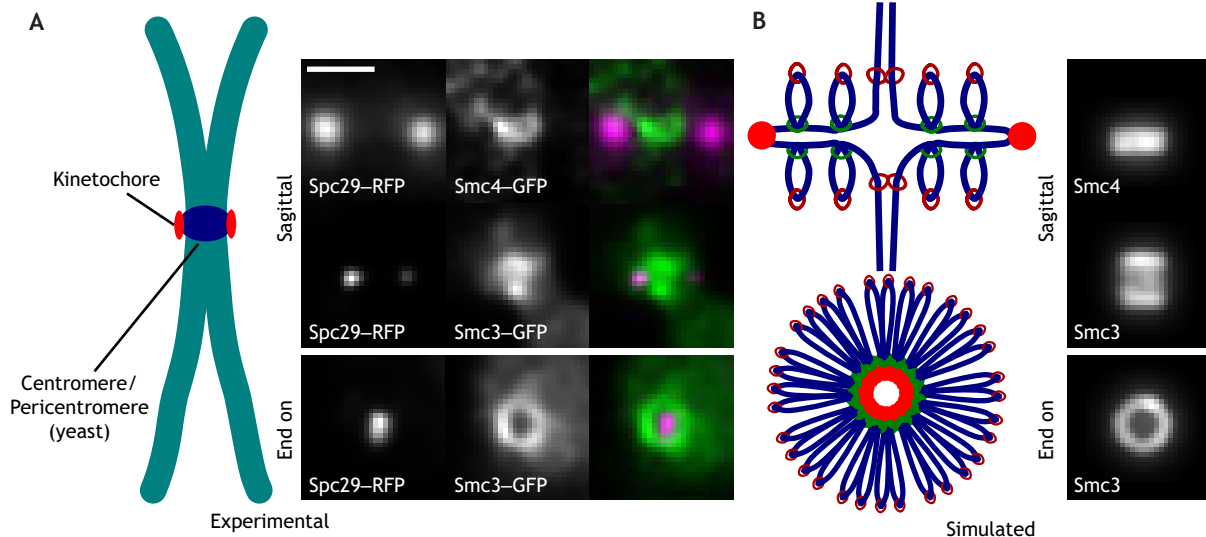


**Fig. 3. Similarities between experimental and simulated images highlight the predictive power of the bottlebrush model.** (A) Schematic of mitotic chromosome. Spatial segregation of condensin and cohesin in a pericentromere during mitosis. Deconvolved, experimental images (taken by Julian Haase) of spindle poles (Spc29, magenta), condensin (SMC4, top, green) and cohesin (SMC3, middle, bottom, green). Distance between spindle poles is ~1–1.5  $\mu\text{m}$ . (B) Schematic illustration of a pair of sister chromatid loops within the pericentromere. Condensin is at the base (green) and cohesin (burgundy) is at the tips of DNA loops (blue). The 125 bp centromere (red ball) is the site of kinetochore assembly in budding yeast (apex of primary, horizontal loops), and sister kinetochores are ~800 nm apart. Simulated images (Sim) from 3D model showing the distribution of SMC4 (top) and SMC3 (middle: sagittal and bottom, end-on view) (Stephens et al., 2013b). Cohesin (Smc3) appears as a barrel in the end-on view because the diameter (500 nm) of the average position of individual cohesin proteins exceeds the diffraction limit (~300 nm). Bottom, end-on view of pericentromeres from all 16 chromosomes in their metaphase configuration. Scale bar: 1  $\mu\text{m}$  (applies to all experimental and simulated images).

which happens to lie approximately midway between the base and the tip of a DNA loop. In this way, the diameter of the cohesin barrel expands as the size of the loops increases. The dimension of the cohesin can be experimentally manipulated, and is dependent on the state of histone H2A phosphorylation (Haase et al., 2012). While the size of individual loops cannot be measured, changes in chromatin structure modulate the DNA persistence length, which contributes to DNA loop size, validating the model predictions.

The displacement of cohesin distal to the spindle axis predicts that pericentromere DNA itself is cylindrically arrayed around the central spindle. Using FROS as markers of the pericentromere, the DNA was found to occupy a region roughly cylindrical in geometry surrounding the central spindle. The mean position of pericentromere DNA overlaps the geometrical position of cohesin (Anderson et al., 2009). This finding rules out simple models of the centromere (Fig. 1A,B) and points to models in which DNA fills the entire space spanning the distance between sister kinetochores (Fig. 1C,D).

It is important to note that the bottlebrush models make no assumptions with regard to the ability of cohesin to link DNA strands. Evidence for non-sister strand linkage is derived from image analysis of FROS arrays on pericentromeres from different chromosomes (Stephens et al., 2013c). Analysis of multiple FROS arrays has revealed correlated movement during metaphase, indicative of physical linkages between different chromosomes. Indeed, implementing cross-linking between adjacent loops of different sister chromatids mediated by cohesin in our model allowed us to account for the extent of the experimentally observed correlated motion (Lawrimore et al., 2016). The bottlebrush model of pericentromeres thus provides the mechanistic basis for experimental observations of their position and dynamics for different chromosomes (Stephens et al., 2013a, 2013c). Therefore, fully understanding the mitotic segregation apparatus requires a conceptual shift by expanding the focus from the well-studied mitotic spindle (i.e. spindle MTs) and kinetochores to include the bottlebrush, which minimally comprises cohesin, condensin and pericentromeric chromatin. It is imperative that we understand how

the mass of pericentromeric chromatin that lies between sister kinetochores is integrated into the mechanism that generates and detects informative tension at the kinetochore.

Kinetochores from each of the 16 yeast chromosomes are visualized as a single diffraction-limited cluster, and upon biorientation in metaphase, they appear as two clusters separated by  $\sim 800$  nm (Pearson et al., 2001). A bottlebrush formed by all of the pericentromeres can explain why all kinetochores cluster together (because cohesin links loops from different pericentromeres into a single bottlebrush) (Ng et al., 2009) and why the sister clusters are 800 nm apart (because this is the length of a bottlebrush that will be stiffened by the number and density of loops available through the size of the pericentromeric DNA) (Xie et al., 2019) (Figs 3 and 4). We postulate that in species with regional centromeres like humans, there is enough centromeric DNA in each chromosome to form a similar ‘bottlebrush’ structure at a single centromere, without need for clustering of kinetochores from different chromosomes (Aze et al., 2016; Lawrimore and Bloom, 2019). Computer simulations predict that tether points at the base of condensin-mediated DNA loops are driven to the axis in the presence of an extensional force such as exerted by spindle MTs (Lawrimore et al., 2016) (Fig. 4A,C). Slip-link tethers such as those mediated by cohesin diffuse along the DNA, where they fluctuate to the radial periphery of DNA loops regardless of whether there is an extensional force. The different chromatin-tethering modalities of cohesin (diffusible slip-links) and condensin (DNA loop extruders), together with the extensional force from spindle MTs, result in their geometric partitioning and provide a mechanism to convert DNA from a floppy polymer into a stiff bottlebrush that can sustain tension across micron-scale distances (Goloborodko et al., 2016; Lawrimore et al., 2016, 2018; Xie et al., 2019).

## Conclusions

In summary, as discussed above, the organization of the pericentromeric chromatin between sister kinetochores of budding yeast closely resembles a bottlebrush polymer. The point centromeres lie at the ends of the brush, where they interact with

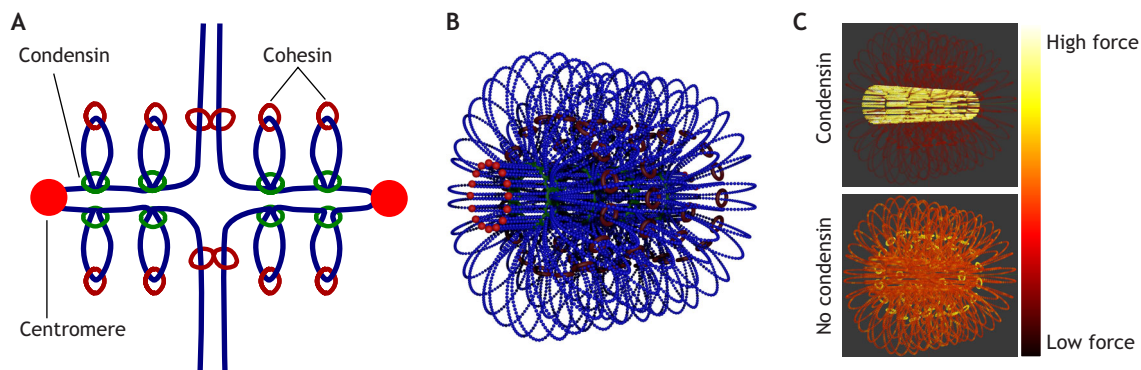


**Fig. 4. The bottlebrush model for a yeast centromere.** (A) Schematic illustration of the pericentromere loops from one pair of sister chromatids. DNA is depicted as blue strands and the distance between sister centromeres is  $\sim 800$  nm. (B) A computational polymer dynamics model that can be directly compared to time-lapse visualization of chromatin through lacO–LacI–GFP and SMC–GFP fusion proteins (Lawrimore et al., 2016). The bottlebrush is generated by the clustering of pericentromere loops from all 16 pairs of sister chromatids in metaphase as shown here, resulting in  $\sim 1$ – $1.6$  Mbp DNA ( $30$ – $50$  kbp/pericentromere  $\times$  two sister strands  $\times$  16 chromosomes). Chromosome arms are not included in the model. (C) Illustration of how the brush focuses tension along spindle axis (Lawrimore et al., 2018). DNA loops sterically repulse one another, exerting a force on the primary axis (from one sister centromere to the other, in A). Force is estimated from the separation between individual beads that make up the bead-spring polymer model, the greater the bead separation, the higher the force (from black to yellow). In the presence of cohesin and condensin (top), force is focused on the primary axis (yellow). In the absence of condensin (bottom), the force is lower and evenly distributed throughout the brush. This lower force is in the sub-picoNewton range and reflects thermal fluctuations. The higher force in both panels (yellow) is on the order of  $5$ – $7$  piconewtons, which is comparable to independent *in vivo* data and *in vitro* measurements of reconstituted kinetochore–microtubule attachment (Chacon et al., 2014; Akiyoshi et al., 2010). This model provides a physical basis for the conservation of distance between separated sister kinetochores, indicating the bottlebrush to be a conserved mechanistic solution to centromere stiffness.

kinetochores. The pericentromere is the 30–50 kb region flanking the point centromere, enriched in cohesin and condensin, and extending to sites of convergent gene transcription. Condensin forms a looped loop DNA structure by extruding loops in the pericentromere. Condensin lies along the spindle axis, coincident with the base of the loops. Cohesin complexes act as slip links that diffuse to the thermodynamically favored position in the loop. Cohesin is radially displaced from the base of the loops and appears as a barrel surrounding the central spindle. Additionally, cohesins may cross-link other cohesin complexes within the pericentromere as evidenced by the correlated motion of non-sister pericentromeres. The bottlebrush model reconciles findings from population studies (ChIP) with live-cell imaging based on the physics of a thermally fluctuating DNA polymer. Cohesin and condensin are spatially segregated in the pericentromere of individual cells. However, these protein complexes bind an overlapping set of DNA sequences due to the fluctuation of DNA to different positions of loops (e.g. base, middle or tip) in different cells. The behavior of single chromatid chains in live cells is necessary to interpret statistical data from population studies. The bottlebrush thus provides the physical basis for how pulling forces from the mitotic spindle are transmitted through the region between sister kinetochores. In budding yeast, 32 disparate chromatids are aggregated into a single stiff structure owing to the loop extrusion and potential cross-linking activities of cohesin and condensin (Ganji et al., 2018; Stephens et al., 2013c; Terakawa et al., 2017). We propose that for both point and regional centromeres, the brush is the biophysical basis for generating tension with a floppy material. Based on the conservation of sister–sister kinetochore separation distance (800 to 1000 nm) (Box 1) and the highly looped nature of regional centromeres, such as occur in humans (Aze et al., 2016), the bottlebrush organization may be conserved across different species as an elegant solution to the problem of generating tension from a floppy and extensible DNA substrate.

#### Acknowledgements

The authors thank Diana Cook, Dr Elaine Yeh (Biology UNC-CH) and Dr M. Greg Forest (Applied Math UNC-CH) for critical comments on the manuscript.

#### Competing interests

The authors declare no competing or financial interests.

#### Funding

This work was funded by National Institutes of General Medical Sciences grant number R37GM32238. Deposited in PMC for release after 12 months.

#### References

- Akiyoshi, B., Sarangapani, K. K., Powers, A. F., Nelson, C. R., Reichow, S. L., Arellano-Santoyo, H., Gonen, T., Ranish, J. A., Asbury, C. L. and Biggins, S. (2010). Tension directly stabilizes reconstituted kinetochore-microtubule attachments. *Nature* **468**, 576–579. doi:10.1038/nature09594
- Alipour, E. and Marko, J. F. (2012). Self-organization of domain structures by DNA-loop-extruding enzymes. *Nucleic Acids Res.* **40**, 11202–11212. doi:10.1093/nar/gks925
- Anderson, M., Haase, J., Yeh, E. and Bloom, K. (2009). Function and assembly of DNA looping, clustering, and microtubule attachment complexes within a eukaryotic kinetochore. *Mol. Biol. Cell* **20**, 4131–4139. doi:10.1091/mbc.e09-05-0359
- Aze, A., Sannino, V., Soffientini, P., Bachi, A. and Costanzo, V. (2016). Centromeric DNA replication reconstitution reveals DNA loops and ATR checkpoint suppression. *Nat. Cell Biol.* **18**, 684–691. doi:10.1038/ncb3344
- Biggins, S. (2013). The composition, functions, and regulation of the budding yeast kinetochore. *Genetics* **194**, 817–846. doi:10.1534/genetics.112.145276
- Blat, Y. and Kleckner, N. (1999). Cohesins bind to preferential sites along yeast chromosome III, with differential regulation along arms versus the centric region. *Cell* **98**, 249–259. doi:10.1016/S0092-8674(00)81019-3
- Bloom, K. S. (2008). Beyond the code: the mechanical properties of DNA as they relate to mitosis. *Chromosoma* **117**, 103–110. doi:10.1007/s00412-007-0138-0

- Bloom, K. S. and Carbon, J. (1982). Yeast centromere DNA is in a unique and highly ordered structure in chromosomes and small circular minichromosomes. *Cell* **29**, 305–317. doi:10.1016/0092-8674(82)90147-7
- Borrie, M. S., Campor, J. S., Joshi, H. and Gartenberg, M. R. (2017). Binding, sliding, and function of cohesin during transcriptional activation. *Proc. Natl Acad. Sci. USA* **114**, E1062–E1071.
- Bustamante, C., Marko, J. F., Siggia, E. D. and Smith, S. (1994). Entropic elasticity of lambda-phage DNA. *Science* **265**, 1599–1600. doi:10.1126/science.8079175
- Bystricky, K., Heun, P., Gehlen, L., Langowski, J. and Gasser, S. M. (2004). Long-range compaction and flexibility of interphase chromatin in budding yeast analyzed by high-resolution imaging techniques. *Proc. Natl. Acad. Sci. USA* **101**, 16495–16500. doi:10.1073/pnas.0402766101
- Chacon, J. M., Mukherjee, S., Schuster, B. M., Clarke, D. J. and Gardner, M. K. (2014). Pericentromere tension is self-regulated by spindle structure in metaphase. *J. Cell Biol.* **205**, 313–324. doi:10.1083/jcb.201312024
- Cherry, L. M., Faulkner, A. J., Grossberg, L. A. and Balczon, R. (1989). Kinetochore size variation in mammalian chromosomes: an image analysis study with evolutionary implications. *J. Cell Sci.* **92**, 281–289. doi:10.1242/jcs.92.2.281
- Cleveland, D. W., Mao, Y. and Sullivan, K. F. (2003). Centromeres and kinetochores: from epigenetics to mitotic checkpoint signaling. *Cell* **112**, 407–421. doi:10.1016/S0092-8674(03)00115-6
- D'Amrosio, C., Schmidt, C. K., Katou, Y., Kelly, G., Itoh, T., Shirahige, K. and Uhlmann, F. (2008). Identification of cis-acting sites for condensin loading onto budding yeast chromosomes. *Genes Dev.* **22**, 2215–2227. doi:10.1101/gad.1675708
- de Gennes, P. G. (1979). *Scaling Concepts in Polymer Physics*. Ithaca, New York: Cornell Univ. Press.
- Dekker, J. and Misteli, T. (2015). Long-range chromatin interactions. *Cold Spring Harb Perspect Biol.* **7**, a019356. doi:10.1101/cshperspect.a019356
- Dekker, J., Marti-Renom, M. A. and Mirny, L. A. (2013). Exploring the three-dimensional organization of genomes: interpreting chromatin interaction data. *Nat. Rev. Genet.* **14**, 390–403. doi:10.1038/nrg3454
- Dewar, H., Tanaka, K., Nasmyth, K. and Tanaka, T. U. (2004). Tension between two kinetochores suffices for their bi-orientation on the mitotic spindle. *Nature* **428**, 93–97. doi:10.1038/nature02328
- Ding, R., McDonald, K. L. and McIntosh, J. R. (1993). Three-dimensional reconstruction and analysis of mitotic spindles from the yeast, *Schizosaccharomyces pombe*. *J. Cell Biol.* **120**, 141–151. doi:10.1083/jcb.120.1.141
- Dion, V. and Gasser, S. M. (2013). Chromatin movement in the maintenance of genome stability. *Cell* **152**, 1355–1364. doi:10.1016/j.cell.2013.02.010
- Doi, M. and Edwards, S. F. (1986). *The Theory of Polymer Dynamics*. Clarendon, Oxford: Oxford University Press.
- Dostie, J. and Bickmore, W. A. (2012). Chromosome organization in the nucleus - charting new territory across the Hi-Cs. *Curr. Opin. Genet. Dev.* **22**, 125–131. doi:10.1016/j.gde.2011.12.006
- Earnshaw, W. C., Halligan, B., Cooke, C. A., Heck, M. M. and Liu, L. F. (1985). Topoisomerase II is a structural component of mitotic chromosome scaffolds. *J. Cell Biol.* **100**, 1706–1715. doi:10.1083/jcb.100.5.1706
- Elbatsh, A. M. O., Kim, E., Eeftens, J. M., Raaijmakers, J. A., van der Weide, R. H., Garcia-Nieto, A., Bravo, S., Ganji, M., Uit de Bos, J., Teunissen, H. et al. (2019). Distinct roles for condensin's two ATPase sites in chromosome condensation. *Mol. Cell* **76**, 724–737.e5. doi:10.1016/j.molcel.2019.09.020
- Ganji, M., Shaltiel, I. A., Bisht, S., Kim, E., Kalichava, A., Haering, C. H. and Dekker, C. (2018). Real-time imaging of DNA loop extrusion by condensin. *Science* **360**, 102–105. doi:10.1126/science.aar7831
- Gardner, M. K., Sprague, B. L., Pearson, C. G., Cosgrove, B. D., Bicek, A. D., Bloom, K., Salmon, E. D. and Odde, D. J. (2010). Model Convolution: A Computational Approach to Digital Image Interpretation. *Cell Mol Bioeng* **3**, 163–170. doi:10.1007/s12195-010-0101-7
- Gibcus, J. H., Samejima, K., Goloborodko, A., Samejima, I., Naumova, N., Nuebler, J., Kanemaki, M. T., Xie, L., Paulson, J. R., Earnshaw, W. C. et al. (2018). A pathway for mitotic chromosome formation. *Science* **359**, eaao6135. doi:10.1126/science.aao6135
- Glynn, E. F., Megee, P. C., Yu, H. G., Mistrot, C., Unal, E., Koshland, D. E., DeRisi, J. L. and Gerton, J. L. (2004). Genome-wide mapping of the cohesin complex in the yeast *Saccharomyces cerevisiae*. *PLoS Biol.* **2**, E259. doi:10.1371/journal.pbio.0020259
- Goloborodko, A., Imakaev, M. V., Marko, J. F. and Mirny, L. (2016). Compaction and segregation of sister chromatids via active loop extrusion. *Elife* **5**, e14864. doi:10.7554/eLife.14864.018
- Goshima, G. and Yanagida, M. (2000). Establishing biorientation occurs with precocious separation of the sister kinetochores, but not the arms, in the early spindle of budding yeast. *Cell* **100**, 619–633. doi:10.1016/S0092-8674(00)80699-6
- Haase, J., Stephens, A., Verdaasdonk, J., Yeh, E. and Bloom, K. (2012). Bub1 kinase and Sgo1 modulate pericentric chromatin in response to altered microtubule dynamics. *Curr. Biol.* **22**, 471–481. doi:10.1016/j.cub.2012.02.006



- Haering, C. H., Lowe, J., Hochwagen, A. and Nasmyth, K.** (2002). Molecular architecture of SMC proteins and the yeast cohesin complex. *Mol. Cell* **9**, 773-788. doi:10.1016/S1097-2765(02)00515-4
- Harasymiw, L. A., Tank, D., McClellan, M., Panigrahy, N. and Gardner, M. K.** (2019). Centromere mechanical maturation during mammalian cell mitosis. *Nat. Commun.* **10**, 1761. doi:10.1038/s41467-019-09578-z
- He, X., Asthana, S. and Sorger, P. K.** (2000). Transient sister chromatid separation and elastic deformation of chromosomes during mitosis in budding yeast. *Cell* **101**, 763-775. doi:10.1016/S0092-8674(00)80888-0
- He, Y., Lawrimore, J., Cook, D., Van Gorder, E. E., De Larimat, S. C., Adalsteinsson, D., Forest, G. M. and Bloom, K.** (2020). Statistical mechanics of chromosomes: in vivo and in silico approaches reveal high-level organization and structure arise exclusively through mechanical feedback between loop extruders and chromatin substrate properties. *Nucleic Acids Res.* **48**, 11284-11303. doi:10.1093/nar/gkaa871
- Henderson, S. A. and Koch, C. A.** (1970). Co-orientation stability by physical tension: a demonstration with experimentally interlocked bivalents. *Chromosoma* **29**, 207-216. doi:10.1007/BF00326079
- Hirano, T.** (2006). At the heart of the chromosome: SMC proteins in action. *Nat. Rev. Mol. Cell Biol.* **7**, 311-322. doi:10.1038/nrm1909
- Howard, J.** (2001). *Mechanics of Motor Proteins and the Cytoskeleton*. Sunderland, Massachusetts: Sinauer Associates, Inc.
- Hult, C., Adalsteinsson, D., Vasquez, P. A., Lawrimore, J., Bennett, M., York, A., Cook, D., Yeh, E., Forest, M. G. and Bloom, K.** (2017). Enrichment of dynamic chromosomal crosslinks drive phase separation of the nucleolus. *Nucleic Acids Res.* **45**, 11159-11173. doi:10.1093/nar/gkx741
- Jannink, G., Duplantier, B. and Sikorav, J. L.** (1996). Forces on chromosomal DNA during anaphase. *Biophys. J.* **71**, 451-465. doi:10.1016/S0006-3495(96)79247-0
- Joglekar, A. P. and Kukreja, A. A.** (2017). How kinetochore architecture shapes the mechanisms of its function. *Curr. Biol.* **27**, R816-R824. doi:10.1016/j.cub.2017.06.012
- Joglekar, A. P., Bouck, D. C., Molk, J. N., Bloom, K. S. and Salmon, E. D.** (2006). Molecular architecture of a kinetochore-microtubule attachment site. *Nat. Cell Biol.* **8**, 581-585. doi:10.1038/ncb1414
- Joglekar, A. P., Bloom, K. and Salmon, E. D.** (2009). In vivo protein architecture of the eukaryotic kinetochore with nanometer scale accuracy. *Curr. Biol.* **19**, 694-699. doi:10.1016/j.cub.2009.02.056
- Jun, S. and Mulder, B.** (2006). Entropy-driven spatial organization of highly confined polymers: lessons for the bacterial chromosome. *Proc. Natl. Acad. Sci. USA* **103**, 12388-12393. doi:10.1073/pnas.0605305103
- Kim, E., Kerssemakers, J., Shaltiel, I. A., Haering, C. H. and Dekker, C.** (2020). DNA-loop extruding condensin complexes can traverse one another. *Nature* **579**, 438-442.
- Kong, M., Cutts, E. E., Pan, D., Beuron, F., Kaliyappan, T., Xue, C., Morris, E. P., Musacchio, A., Vannini, A. and Greene, E. C.** (2020). Human condensin I and II drive extensive ATP-dependent compaction of nucleosome-bound DNA. *Mol. Cell* **79**, 99-114.e9. doi:10.1016/j.molcel.2020.04.026
- Kruthof, M., Chien, F.-T., Routh, A., Logie, C., Rhodes, D. and van Noort, J.** (2009). Single-molecule force spectroscopy reveals a highly compliant helical folding for the 30-nm chromatin fiber. *Nat. Struct. Mol. Biol.* **16**, 534-540. doi:10.1038/nsmb.1590
- Kukreja, A. A., Kavuri, S. and Joglekar, A. P.** (2020). Microtubule attachment and centromeric tension shape the protein architecture of the human kinetochore. *Curr. Biol.* **30**, 4869-4881.e5. doi:10.1016/j.cub.2020.09.038
- Lawrimore, J. and Bloom, K.** (2019). The regulation of chromosome segregation via centromere loops. *Crit. Rev. Biochem. Mol. Biol.* **54**, 352-370. doi:10.1080/10409238.2019.1670130
- Lawrimore, J., Bloom, K. S. and Salmon, E. D.** (2011). Point centromeres contain more than a single centromere-specific Cse4 (CENP-A) nucleosome. *J. Cell Biol.* **195**, 573-582. doi:10.1083/jcb.201106036
- Lawrimore, J., Vasquez, P. A., Falvo, M. R., Taylor, R. M., II, Vicci, L., Yeh, E., Forest, M. G. and Bloom, K.** (2015). DNA loops generate intracentromere tension in mitosis. *J. Cell Biol.* **210**, 553-564. doi:10.1083/jcb.201502046
- Lawrimore, J., Aicher, J. K., Hahn, P., Fulp, A., Kompa, B., Vicci, L., Falvo, M., Taylor, R. M., II and Bloom, K.** (2016). ChromoShake: a chromosome dynamics simulator reveals that chromatin loops stiffen centromeric chromatin. *Mol. Biol. Cell* **27**, 153-166. doi:10.1091/mbc.E15-08-0575
- Lawrimore, J., Barry, T. M., Barry, R. M., York, A. C., Friedman, B., Cook, D. M., Akielis, K., Tyler, J., Vasquez, P., Yeh, E. et al.** (2017a). Microtubule dynamics drive enhanced chromatin motion and mobilize telomeres in response to DNA damage. *Mol. Biol. Cell* **28**, 1701-1711. doi:10.1091/mbc.e16-12-0846
- Lawrimore, J., Friedman, B., Doshi, A. and Bloom, K.** (2017b). RotoStep: a chromosome dynamics simulator reveals mechanisms of loop extrusion. *Cold Spring Harbor Symp. Quant. Biol.* **82**, 101-109. doi:10.1101/sqb.2017.82.033696
- Lawrimore, J., Doshi, A., Friedman, B., Yeh, E. and Bloom, K.** (2018). Geometric partitioning of cohesin and condensin is a consequence of chromatin loops. *Mol. Biol. Cell* **29**, 2737-2750. doi:10.1091/mbc.E18-02-0131
- Lawrimore, J., Kolbin, D., Stanton, J., Khan, M., de Larminat, S. C., Lawrimore, C., Yeh, E. and Bloom, K.** (2021). The rDNA is biomolecular condensate formed by polymer-polymer phase separation and is sequestered in the nucleolus by transcription and R-loops. *Nucleic Acids Res.* **49**, 4586-4598. doi:10.1093/nar/gkab229
- Lebedeva, N. V., Nese, A., Sun, F. C., Matyjaszewski, K. and Sheiko, S. S.** (2012). Anti-Arrhenius cleavage of covalent bonds in bottlebrush macromolecules on substrate. *Proc. Natl. Acad. Sci. USA* **109**, 9276-9280. doi:10.1073/pnas.1118517109
- Li, X. and Nicklas, R. B.** (1995). Mitotic forces control a cell-cycle checkpoint. *Nature* **373**, 630-632. doi:10.1038/373630a0
- Maddox, P. S., Portier, N., Desai, A. and Oegema, K.** (2006). Molecular analysis of mitotic chromosome condensation using a quantitative time-resolved fluorescence microscopy assay. *Proc. Natl. Acad. Sci. USA* **103**, 15097-15102. doi:10.1073/pnas.0606993103
- Maresca, T. J. and Salmon, E. D.** (2009). Intrakinetochores stretch is associated with changes in kinetochore phosphorylation and spindle assembly checkpoint activity. *J. Cell Biol.* **184**, 373-381. doi:10.1083/jcb.200808130
- Marko, J. F. and Siggia, E. D.** (1995). Stretching DNA. *Macromolecules* **28**, 8759-8770. doi:10.1021/ma00130a008
- Mascarenhas, J., Soppa, J., Strunnikov, A. V. and Graumann, P. L.** (2002). Cell cycle-dependent localization of two novel prokaryotic chromosome segregation and condensation proteins in *Bacillus subtilis* that interact with SMC protein. *EMBO J.* **21**, 3108-3118. doi:10.1093/emboj/cdf314
- Megee, P. C., Mistrot, C., Guacci, V. and Koshland, D.** (1999). The centromeric sister chromatid cohesion site directs Mcd1p binding to adjacent sequences. *Mol. Cell* **4**, 445-450. doi:10.1016/S1097-2765(00)80347-0
- Mellone, B. G. and Fachinetti, D.** (2021). Diverse mechanisms of centromere specification. *Curr. Biol.* **31**, R1491-r1504. doi:10.1016/j.cub.2021.09.083
- Michaëlis, C., Ciosk, R. and Nasmyth, K.** (1997). Cohesins: chromosomal proteins that prevent premature separation of sister chromatids. *Cell* **91**, 35-45. doi:10.1016/S0092-8674(01)80007-6
- Miga, K. H. and Sullivan, B. A.** (2021). Expanding studies of chromosome structure and function in the era of T2T genomics. *Hum. Mol. Genet.* **30**, R198-r205. doi:10.1093/hmg/ddab025
- Miga, K. H., Koren, S., Rhie, A., Vollger, M. R., Gershman, A., Bzikadze, A., Brooks, S., Howe, E., Porubsky, D., Logsdon, G. A. et al.** (2020). Telomere-to-telomere assembly of a complete human X chromosome. *Nature* **585**, 79-84. doi:10.1038/s41586-020-2547-7
- Mirny, L. A.** (2011). The fractal globule as a model of chromatin architecture in the cell. *Chromosome Res.* **19**, 37-51. doi:10.1007/s10577-010-9177-0
- Mitchison, T. J. and Salmon, E. D.** (2001). Mitosis: a history of division. *Nat. Cell Biol.* **3**, E17-E21. doi:10.1038/35050656
- Mukherjee, S., Sandri, B. J., Tank, D., McClellan, M., Harasymiw, L. A., Yang, Q., Parker, L. L. and Gardner, M. K.** (2019). A gradient in metaphase tension leads to a scaled cellular response in mitosis. *Dev. Cell* **49**, 63-76.e10. doi:10.1016/j.devcel.2019.01.018
- Musacchio, A. and Ciliberto, A.** (2012). The spindle-assembly checkpoint and the beauty of self-destruction. *Nat. Struct. Mol. Biol.* **19**, 1059-1061. doi:10.1038/nsmb.2429
- Musacchio, A. and Desai, A.** (2017). A molecular view of kinetochore assembly and function. *Biology* **6**, 5. doi:10.3390/biology6010005
- Nasmyth, K. and Haering, C. H.** (2009). Cohesin: its roles and mechanisms. *Annu. Rev. Genet.* **43**, 525-558. doi:10.1146/annurev-genet-102108-134233
- Ng, T. M., Waples, W. G., Lavoie, B. D. and Biggins, S.** (2009). Pericentromeric sister chromatid cohesion promotes kinetochore biorientation. *Mol. Cell* **20**, 3818-3827. doi:10.1091/mbc.e09-04-0330
- Nicklas, R. B.** (1983). Measurements of the force produced by the mitotic spindle in anaphase. *J. Cell Biol.* **97**, 542-548. doi:10.1083/jcb.97.2.542
- Nicklas, R. B.** (1988). The forces that move chromosomes in mitosis. *Annu. Rev. Biophys. Chem.* **17**, 431-449. doi:10.1146/annurev.bb.17.060188.002243
- Nicklas, R. B. and Koch, C. A.** (1969). Chromosome micromanipulation. 3. Spindle fiber tension and the reorientation of mal-oriented chromosomes. *J. Cell Biol.* **43**, 40-50. doi:10.1083/jcb.43.1.40
- Nicklas, R. B., Ward, S. C. and Gorbsky, G. J.** (1995). Kinetochore chemistry is sensitive to tension and may link mitotic forces to a cell cycle checkpoint. *J. Cell Biol.* **130**, 929-939. doi:10.1083/jcb.130.4.929
- Okumura, Y. and Ito, K.** (2001). The polyrotaxane gel: a topological gel by figure-of-eight cross-links. *Adv. Mater.* **13**, 485-487. doi:10.1002/1521-4095(200104)13:7<485::AID-ADMA485>3.0.CO;2-T
- Ou, H. D., Phan, S., Deerinck, T. J., Thor, A., Ellisman, M. H. and O'Shea, C. C.** (2017). ChromEMT: Visualizing 3D chromatin structure and compaction in interphase and mitotic cells. *Science* **357**, 370-382. doi:10.1126/science.aag0025
- Paldi, F., Alver, B., Robertson, D., Schalbetter, S. A., Kerr, A., Kelly, D. A., Baxter, J., Neale, M. J. and Marston, A. L.** (2020). Convergent genes shape budding yeast pericentromeres. *Nature* **582**, 119-123. doi:10.1038/s41586-020-2244-6
- Panyukov, S., Zhulina, E. B., Sheiko, S. S., Randall, G. C., Brock, J. and Rubinstein, M.** (2009a). Tension amplification in molecular brushes in solutions and on substrates (dagger). *J. Phys. Chem. B* **113**, 12. doi:10.1021/jp807671b

- Panyukov, S. V., Sheiko, S. S. and Rubinstein, M.** (2009b). Amplification of tension in branched macromolecules. *Phys. Rev. Lett.* **102**, 148301. doi:10.1103/PhysRevLett.102.148301
- Paulson, J. R. and Laemmli, U. K.** (1977). The structure of histone-depleted metaphase chromosomes. *Cell* **12**, 817-828. doi:10.1016/0092-8674(77)90280-X
- Pearson, C. G., Maddox, P. S., Salmon, E. D. and Bloom, K.** (2001). Budding yeast chromosome structure and dynamics during mitosis. *J. Cell Biol.* **152**, 1255-1266. doi:10.1083/jcb.152.6.1255
- Quammen, C. W., Richardson, A. C., Haase, J., Harrison, B. D., Taylor, R. M. and Bloom, K. S.** (2008). FluoroSim: a visual problem-solving environment for fluorescence microscopy. *Eurographics Workshop Vis. Comput. Biomed.* **2008**, 151-158.
- Robinett, C. C., Straight, A., Li, G., Wilhelm, C., Sudlow, G., Murray, A. and Belmont, A. S.** (1996). In vivo localization of DNA sequences and visualization of large-scale chromatin organization using lac operator/repressor recognition. *J. Cell Biol.* **135**, 1685-1700. doi:10.1083/jcb.135.6.1685
- Rubinstein, M. and Colby, R. H.** (2003). *Polymer Physics*. Oxford: Oxford University Press.
- Ryu, J.-K., Bouchoux, C., Liu Hon, W., Kim, E., Minamino, M., de Groot, R., Katan Allard, J., Bonato, A., Marenduzzo, D., Michieletto, D. et al.** (2021). Bridging-induced phase separation induced by cohesin SMC protein complexes. *Sci. Adv.* **7**, eabe5905. doi:10.1126/sciadv.abe5905
- Salmon, E. D.** (1975). Pressure-induced depolymerization of spindle microtubules. II. Thermodynamics of in vivo spindle assembly. *J. Cell Biol.* **66**, 114-127. doi:10.1083/jcb.66.1.114
- Salmon, E. D. and Bloom, K.** (2017). Tension sensors reveal how the kinetochore shares its load. *BioEssays* **39**, 10.1002/bies.201600216. doi:10.1002/bies.201600216
- Salmon, E. D., Goode, D., Maugel, T. K. and Bonar, D. B.** (1976). Pressure-induced depolymerization of spindle microtubules. III. Differential stability in HeLa cells. *J. Cell Biol.* **69**, 443-454. doi:10.1083/jcb.69.2.443
- Stephens, A. D., Haase, J., Vicci, L., Taylor, R. M., II and Bloom, K.** (2011). Cohesin, condensin, and the intramolecular centromere loop together generate the mitotic chromatin spring. *J. Cell Biol.* **193**, 1167-1180. doi:10.1083/jcb.201103138
- Stephens, A. D., Haggerty, R. A., Vasquez, P. A., Vicci, L., Snider, C. E., Shi, F., Quammen, C., Mullins, C., Haase, J., Taylor, R. M. II et al.** (2013a). Pericentric chromatin loops function as a nonlinear spring in mitotic force balance. *J. Cell Biol.* **200**, 757-772. doi:10.1083/jcb.201208163
- Stephens, A. D., Quammen, C. W., Chang, B., Haase, J., Taylor, R. M., II and Bloom, K.** (2013b). The spatial segregation of pericentric cohesin and condensin in the mitotic spindle. *Mol. Biol. Cell* **24**, 3909-3919. doi:10.1091/mbc.e13-06-0325
- Stephens, A. D., Snider, C. E., Haase, J., Haggerty, R. A., Vasquez, P. A., Forest, M. G. and Bloom, K.** (2013c). Individual pericentromeres display coordinated motion and stretching in the yeast spindle. *J. Cell Biol.* **203**, 407-416. doi:10.1083/jcb.201307104
- Stigler, J., Çamdere, G. Ö., Koshland, D. E. and Greene, E. C.** (2016). Single-Molecule Imaging Reveals a Collapsed Conformational State for DNA-Bound Cohesin. *Cell Reports* **15**, 988-998. doi:10.1016/j.celrep.2016.04.003
- Straight, A. F., Belmont, A. S., Robinett, C. C. and Murray, A. W.** (1996). GFP tagging of budding yeast chromosomes reveals that protein-protein interactions can mediate sister chromatid cohesion. *Curr. Biol.* **6**, 1599-1608. doi:10.1016/S0960-9822(02)70783-5
- Strick, T. R., Kawaguchi, T. and Hirano, T.** (2004). Real-time detection of single-molecule DNA compaction by condensin I. *Curr. Biol.* **14**, 874-880. doi:10.1016/j.cub.2004.04.038
- Strunnikov, A. V., Larionov, V. L. and Koshland, D.** (1993). SMC1: an essential yeast gene encoding a putative head-rod-tail protein is required for nuclear division and defines a new ubiquitous protein family. *J. Cell Biol.* **123**, 1635-1648. doi:10.1083/jcb.123.6.1635
- Strunnikov, A. V., Hogan, E. and Koshland, D.** (1995). SMC2, a *Saccharomyces cerevisiae* gene essential for chromosome segregation and condensation, defines a subgroup within the SMC family. *Genes Dev.* **9**, 587-599. doi:10.1101/gad.9.5.587
- Talbert, P. B. and Henikoff, S.** (2020). What makes a centromere? *Exp. Cell Res.* **389**, 111895. doi:10.1016/j.yexcr.2020.111895
- Tanaka, T., Fuchs, J., Loidl, J. and Nasmyth, K.** (2000). Cohesin ensures bipolar attachment of microtubules to sister centromeres and resists their precocious separation. *Nat. Cell Biol.* **2**, 492-499. doi:10.1038/35019529
- Terakawa, T., Bisht, S., Eeftens, J. M., Dekker, C., Haering, C. H. and Greene, E. C.** (2017). The condensin complex is a mechanochemical motor that translocates along DNA. *Science* **358**, 672-676. doi:10.1126/science.aan6516
- Underhill, P. T. and Doyle, P. S.** (2004). On the coarse-graining of polymers into bead-spring chains. *J. Non-Newtonian Fluid Mech.* **122**, 3-31. doi:10.1016/j.jnnfm.2003.10.006
- Vasquez, P. A. and Bloom, K.** (2014). Polymer models of interphase chromosomes. *Nucleus* **5**, 376-390. doi:10.4161/nucl.36275
- Vasquez, P. A., Hult, C., Adalsteinsson, D., Lawrimore, J., Forest, M. G. and Bloom, K.** (2016). Entropy gives rise to topologically associating domains. *Nucleic Acids Res.* **44**, 5540-5549. doi:10.1093/nar/gkw510
- Venkei, Z., Przewłoka, M. R., Ladak, Y., Albadri, S., Sossick, A., Juhasz, G., Novak, B. and Glover, D. M.** (2012). Spatiotemporal dynamics of Spc105 regulates the assembly of the *Drosophila* kinetochore. *Open Biol.* **2**, 110032. doi:10.1098/rsob.110032
- Verdaasdonk, J. S., Vasquez, P. A., Barry, R. M., Barry, T., Goodwin, S., Forest, M. G. and Bloom, K.** (2013). Centromere tethering confines chromosome domains. *Mol. Cell* **52**, 819-831. doi:10.1016/j.molcel.2013.10.021
- Wan, X., O'Quinn, R. P., Pierce, H. L., Joglekar, A. P., Gall, W. E., DeLuca, J. G., Carroll, C. W., Liu, S. T., Yen, T. J., McEwen, B. F. et al.** (2009). Protein architecture of the human kinetochore microtubule attachment site. *Cell* **137**, 672-684. doi:10.1016/j.cell.2009.03.035
- Waters, J. C., Skibbens, R. V. and Salmon, E. D.** (1996). Oscillating mitotic newt lung cell kinetochores are, on average, under tension and rarely push. *J. Cell Sci.* **109**, 2823-2831. doi:10.1242/jcs.109.12.2823
- Weber, S. A., Gerton, J. L., Polancic, J. E., DeRisi, J. L., Koshland, D. and Megee, P. C.** (2004). The kinetochore is an enhancer of pericentric cohesin binding. *PLoS Biol.* **2**, E260. doi:10.1371/journal.pbio.0020260
- Winey, M. and Bloom, K.** (2012). Mitotic spindle form and function. *Genetics* **190**, 1197-1224. doi:10.1534/genetics.111.128710
- Xie, G., Martinez, M. R., Olszewski, M., Sheiko, S. S. and Matyjaszewski, K.** (2019). Molecular Bottlebrushes as Novel Materials. *Biomacromolecules* **20**, 27-54. doi:10.1021/acs.biomac.8b01171
- Yan, J., Maresca, T. J., Skoko, D., Adams, C. D., Xiao, B., Christensen, M. O., Heald, R. and Marko, J. F.** (2007). Micromanipulation studies of chromatin fibers in *Xenopus* egg extracts reveal ATP-dependent chromatin assembly dynamics. *Mol. Biol. Cell* **18**, 464-474. doi:10.1091/mbc.e06-09-0800
- Yeh, E., Haase, J., Paliulis, L. V., Joglekar, A., Bond, L., Bouck, D., Salmon, E. D. and Bloom, K. S.** (2008). Pericentric chromatin is organized into an intramolecular loop in mitosis. *Curr. Biol.* **18**, 81-90. doi:10.1016/j.cub.2007.12.019